JACS
JOURNAL OF THE AMERICAN CHEMICAL SOCIETY

ARTICLE

pubs.acs.org/JACS

Engineering Solid-State Morphologies in Carbazole−Ethynylene Macrocycles

Aaron D. Finke,[†] Dustin E. Gross, Amy Han, and Jeffrey S. Moore*

Department of Chemistry, University of Illinois at Urbana-Champaign, 600 South Mathews Avenue, Urbana, Illinois 61801, United States

Supporting Information

ABSTRACT: We present a crystallographic study that systematically investigates the effects of the *n*-alkyl side-chain length on the crystal packing in shape-persistent macrocycles. The solid-state packing of carbazole−ethynylene-containing macrocycles is sensitive to the alkyl-chain length. In macrocycles containing *n*-alkyl side chains up to nine carbons in length, face-on aromatic π interactions predominate, while the addition of one carbon leads to a completely different packing arrangement. Macrocycles with C_{10} or C_{11} chains exhibit a novel packing motif wherein the alkyl chains intercalate between macrocycles, leading in one case to continuous solvent-filled channels. When crystals of the C_{10} macrocycle are bathed in solvent, the included molecules exchange with the external solvent, and the alkyl chain disorder changes in response to changes in the guest volume in order to retain crystallinity. Powder X-ray diffraction data indicate that alkyl−macrocycle interactions in the longer chains "emulate" the distances typical of face-to-face π interactions, leading to deceptive indicators of π stacking.

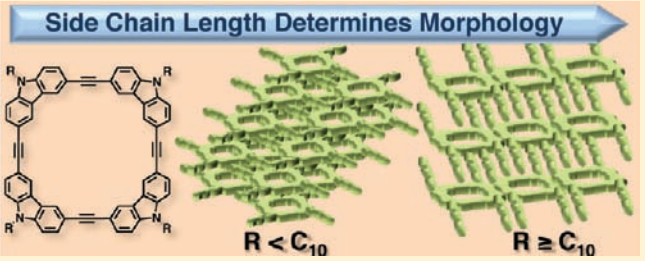

INTRODUCTION

In the world of molecular electronics, where polymeric architectures have dominated the chemical space, discrete small molecules are starting to find their own place as uniquely effective materials.[1−5] Among architectures found in the small-molecule regime, shape-persistent macrocycles (SPMs) constitute a distinct class of architectures whose materials properties can emulate those of high polymers, but with better control of solid-state organization.[6−11] The use of SPMs as functional materials has benefited from recent advancements in their preparative methods.[12−15] Traditionally, widespread utilization of SPMs was hindered by tedious preparation, often requiring dilute conditions, small scales, and difficult separations. The recent implementation of methodologies wherein the bond-formation event is under thermodynamic control, otherwise known as dynamic covalent chemistry, has enabled a diverse array of macrocycles to be generated from simple precursors in a less synthetically demanding manner.[16,17] Advancing the original work of Bunz,[18,19] our laboratory has developed an alkyne-metathesis-based approach to the dynamic covalent formation of arylene−ethynylene macrocycles. This method has also proven useful and efficient for large-scale preparations.[20−22]

The functional applications of many conjugated systems are directly tied to their solid-state packing; thus, rigorous characterization of functional small molecules in the solid state is critical for optimization of their bulk properties.[23] Despite major efforts, the development of molecular design rules to relate chemical identity to a particular solid-state organization remains difficult. Each component of a molecule contributes to geometric constraints and intermolecular interactions.[24] For example, the attachment of alkyl chains to large aromatic moieties is typically utilized to enhance solubility and ease of processing. However, such derivatization can lead to a dramatic change in the solid-state properties. One such example reported by Anthony is the functionalization of pentacene with silylalkynes, which changes the solid-state packing from the orthogonal "herringbone" motif to one in which cofacial interactions are dominant, leading to an increase in the solid-state charge-carrier mobility.[25,26]

One major advantage of using functional small molecules instead of heterogeneous polymeric materials is the ability to explore intermolecular interactions systematically and with high resolution using X-ray crystallography. The first arylene−ethynylene macrocycle characterized by X-ray crystallography, a *m*-phenylene−ethynylene [6]cycle bearing phenol groups, assembles to form porous cavities generated by intermolecular hydrogen bonding in two-dimensional (2D) layers.[27] Subsequent crystallographic investigations of SPMs have demonstrated a significant diversity in the solid-state packing of this class of materials.[18,28−34]

In this article, we present an extensive crystallographic investigation of SPMs containing a carbazole−ethynylene backbone (**1**) (Figure 1). We recently discovered that SPMs of this type readily form nanofibril aggregates whose fluorescence is rapidly quenched in the presence of explosive vapors such as TNT and DNMB.[35] It has been proposed that the quenching event is due to electron transfer from the electron-rich π-stacked macrocycles to the electron-deficient explosive compound.

Received: May 25, 2011
Published: July 20, 2011

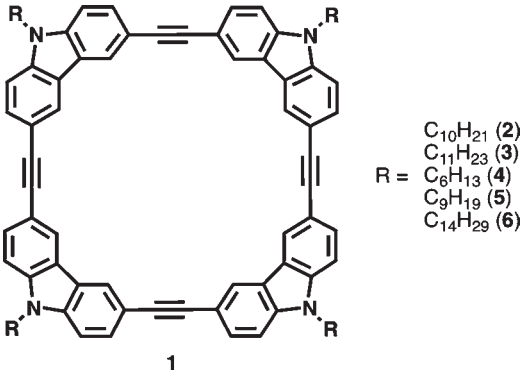

Figure 1. Carbazole−ethynylene macrocycle **1** with various alkyl chains **2**−**6**.

However, the atomistic details of these interactions have not been rigorously determined with high-resolution structure determination methods. Moreover, we sought to probe the effects of alkyl-chain length in a systematic way. Herein we demonstrate using X-ray crystallographic analysis that the packing of **1** in the solid state is quite sensitive to the choice of side chain, leading to the formation of a diverse array of morphologies, some of which are novel to SPMs.

RESULTS

Macrocycles **2**−**6** were prepared via precipitation-driven alkyne metathesis of precursors bearing functionalities whose byproducts precipitate from solution upon cross-metathesis, a process developed in our laboratory (Scheme 1).[21] The synthetic protocol is modular and allows for a variety of monomer units with differing alkyl chains to be prepared in a straightforward manner. Following Fürstner's reports,[36,37] we have found that Mo alkylidynes bearing triphenylsilyloxy ligands are superior alkyne metathesis catalysts for the preparation of macrocycles **1**, exhibiting greater efficiency and tolerance than previously used catalysts bearing electron-deficient phenoxy ligands. The macrocyclization yields were generally good. As expected, the solubilities of the macrocycles were highly dependent on the identity of the alkyl chain; longer alkyl chains led to better solubility of the material.

Crystals suitable for X-ray diffraction were obtained by slow diffusion of ether into solutions of **2**−**5** in a halogenated solvent [typically dichloromethane (DCM)] at room temperature over several days. The crystals were uniform in quality, without apparent polymorphism (except for **2**). The lack of *ordered* heavy atoms ($Z > 8$) in **1** precluded the use of Mo radiation for all but the largest of crystals; the use of Cu sources was required for the others.[38] A summary of the crystallographic data is presented in Table 1.

Crystals of the C_{10}[4]cycle. Crystals of **2** formed in two distinct morphologies: long, thin rods (**2a**·DCM), which contain one long crystal axis, and hexagonal plates (**2b**), which contain two long crystal axes. Crystals of **2a**·DCM were indefinitely stable after removal from solution; in contrast, **2b** rapidly decomposed upon removal from solution, becoming striated within a few minutes and opaque within 1 h. However, crystals of **2b** were stable when immersed in inert oil and rapidly cooled to −100 °C.

The predominant polymorph of the C_{10}[4]cycle, rods **2a**·DCM, crystallized in the monoclinic space group $P2_1$. The macrocycle is mostly planar with a macrocycle plane deviation of 0.10 Å.[39] The four alkyl chains are grouped into two sets of two on the basis of their relative orientation with respect to the macrocycle. The molecule as a whole, including the two sets of alkyl chains and the macrocycle, adopts a chairlike orientation, with each set of alkyl chains propagating nearly perpendicular to the macrocycle plane. The packing consists of two stacks of parallel macrocycles whose macrocycle planes intersect at an angle of 75.5° (Figure 2a). The macrocycle planes are parallel to the crystallographic *a* axis, forming macrocycle rows. Along the *b* axis, there are alternating stacks of macrocycles and alkyl chains; the alkyl chains are also arranged in parallel rows propagating down the *a* axis. The distance between two macrocycles in **2a** is 7.23 Å as a result of the alternating alkyl chain/macrocycle packing. The ends of two of the alkyl chains on one side are slightly disordered. Rows of macrocycles are not parallel down the *c* axis, leading to a "staggered" arrangement that appears as pleated sheets. Macrocycle staggering results in an A−B stacking

Scheme 1. General Synthetic Scheme for the Preparation of Macrocycles 1

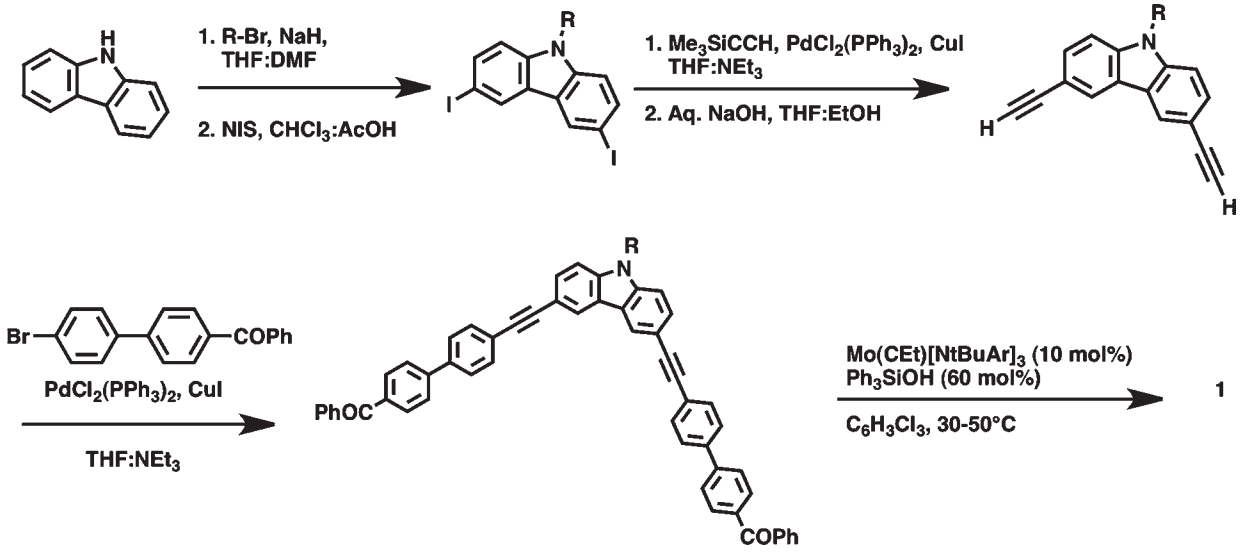

Table 1. Crystallographic Data for All Compounds

	2a·DCM	**2a**·MeOH	**2b**	**3**	**4**·DCM	**4**·DCE	**5**
moiety formula	$C_{96}H_{108}N_4$·(CH_2Cl_2)	$C_{96}H_{108}N_4$·(CH_3OH)	$C_{96}H_{108}N_4$·2(CH_2Cl_2)	$C_{100}H_{116}N_4$	$C_{80}H_{76}N_4$·2(CH_2Cl_2)	$C_{80}H_{76}N_4$·$C_2H_4Cl_2$	$C_{92}H_{100}N_4$
space group	$P2_1$	$P2_1$	$C2/c$	Cc	$P\bar{1}$	$P\bar{1}$	$P\bar{1}$
a (Å)	19.3461(6)	19.4024(7)	42.960(17)	19.277(3)	9.0398(9)	9.2308(4)	9.6728(2)
b (Å)	8.9264(3)	8.9759(3)	9.082(4)	48.012(7)	14.0715(13)	13.2487(6)	12.2684(2)
c (Å)	24.7549(8)	24.5083(7)	24.092(10)	10.382(2)	14.9754(14)	15.2331(7)	15.8148(3)
α (deg)	90	90	90	90	68.419(3)	68.242(2)	95.9930(10)
β (deg)	105.939(2)	106.389(3)	105.579(11)	122.58	77.031(3)	74.840(2)	98.7200(10)
γ (deg)	90	90	90	90	73.791(4)	75.250(2)	102.3650(10)
V (Å^3)	4110.6(2)	4094.8(2)	9055(7)	8096(2)	1685.1(3)	1643.98(13)	1793.71
Z	2	2	4	4	1	1	1
D_{calcd} (g cm^{-1})	1.065	1.070	1.091	1.127	1.245	1.204	1.168
T (K)	100	100	193	173	120	100	100
total reflns	30444	23349	68724	37445	33246	18509	10274
ind. reflns	7630	7383	8238	9823	7441	5777	4346
$R(F)$ $[I > 2\sigma(I)]$[a]	0.0877	0.0892	0.0567	0.0450	0.0531	0.0484	0.0952
$R_w(F^2)$ (all data)[b]	0.2442	0.2529	0.1564	0.1183	0.1552	0.1383	0.2814
GOF S	1.063	1.038	0.903	1.029	1.045	1.043	1.050
MC plane deviation (Å)[c]	0.1001	0.1126	0.0770	0.1789	0.0548	0.1134; 0.2154[d]	0.0783
disordered solvent volume (Å^3)[e]	332	266	1347	n/a	n/a	n/a	n/a

[a] $R(F) = \Sigma||F_o| - |F_c||/\Sigma|F_o|$ for $F_o^2 > 2\sigma(F_o)^2$. [b] $R_w(F_o^2) = [\Sigma w(F_o^2 - F_c^2)^2/\Sigma wF_o^4]^{1/2}$, where $w^{-1} = \sigma^2(F_o)^2 + [M(F_o^2)]^2 + [N(F_o^2 + 2F_c^2)/3]$ for $F_o^2 \geq 0$ and $w^{-1} = \sigma^2(F_o^2)$ for $F_o^2 < 0$. M and N are weighting variables. [c] The macrocycle (MC) plane is the least-squares plane of the macrocycle atoms, not including hydrogens or pendant alkyl chains. The MC plane deviation is the standard deviation from the MC plane for all of the atoms that define it. [d] Each value corresponds to a disorder in one carbazole of the macrocycle. [e] The total disordered solvent-containing volume per unit cell as calculated using SQUEEZE/PLATON.

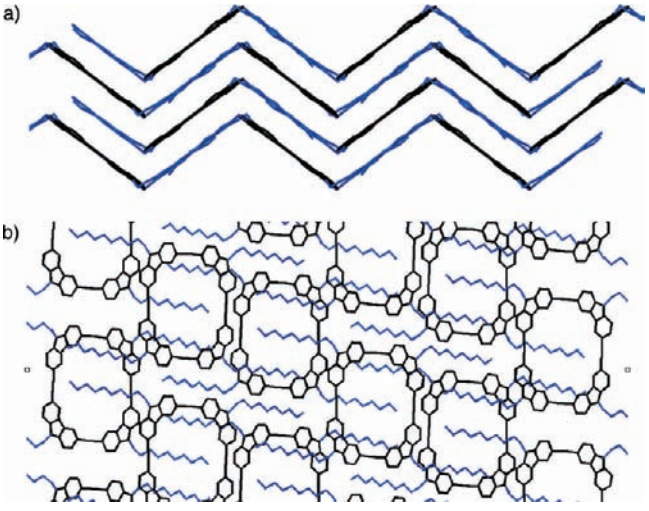

Figure 2. Packing of **2a**·DCM looking down (a) the crystallographic *a* axis and (b) the crystallographic *b* axis. H atoms have been omitted for clarity. In (b), alkyl chains are shown in blue and macrocycles in black.

repeat of the pleated sheets. Importantly, a consequence of this arrangement is that an alkyl chain lies above and below each macrocycle (Figure 2). This arrangement turns out to be critical for understanding solvent effects in the crystal.

The interior cavity of each macrocycle contains one disordered DCM molecule. The solvent positions in **2a** could not be accurately determined, and thus, the electron density present in the disordered solvent regions was removed using the solvent bypass ("SQUEEZE") procedure in the PLATON program.[40]

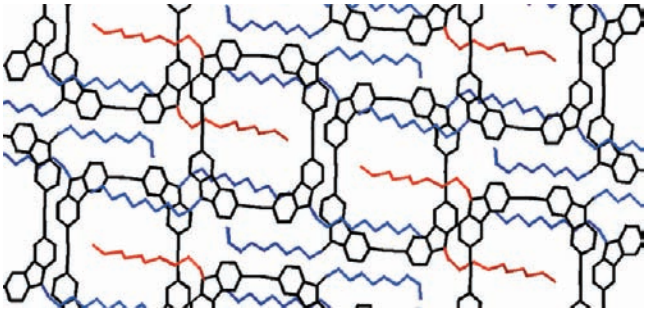

Figure 3. Packing of **2a**·MeOH viewed down the crystallographic *b* axis. Highly disordered alkyl chains are shown in red, other alkyl chains in blue, and macrocycles in black. H atoms have been omitted for clarity.

Despite the fact that **2a** contains free, disordered solvent, the crystals *do not* decompose even after several weeks of sitting in oil under ambient conditions. This could be due to several factors: the solvent may be "trapped" in the macrocycle cavity and thus be unable to escape; alternatively, if the solvent were to escape, the overall crystallinity would not be affected and the resulting void space would be filled by something else.

The following experiment illustrates that both of the above factors may be in play. Crystals of **2a** were immersed in methanol for several weeks; the resulting crystals **2a**·MeOH were then characterized by X-ray diffraction. The DCM was replaced by disordered MeOH, as evidenced by the electron count given by SQUEEZE; as in the case of **2a**, the solvent positions in **2a**·MeOH could not be accurately determined, and thus, the electron density present in the disordered solvent regions was

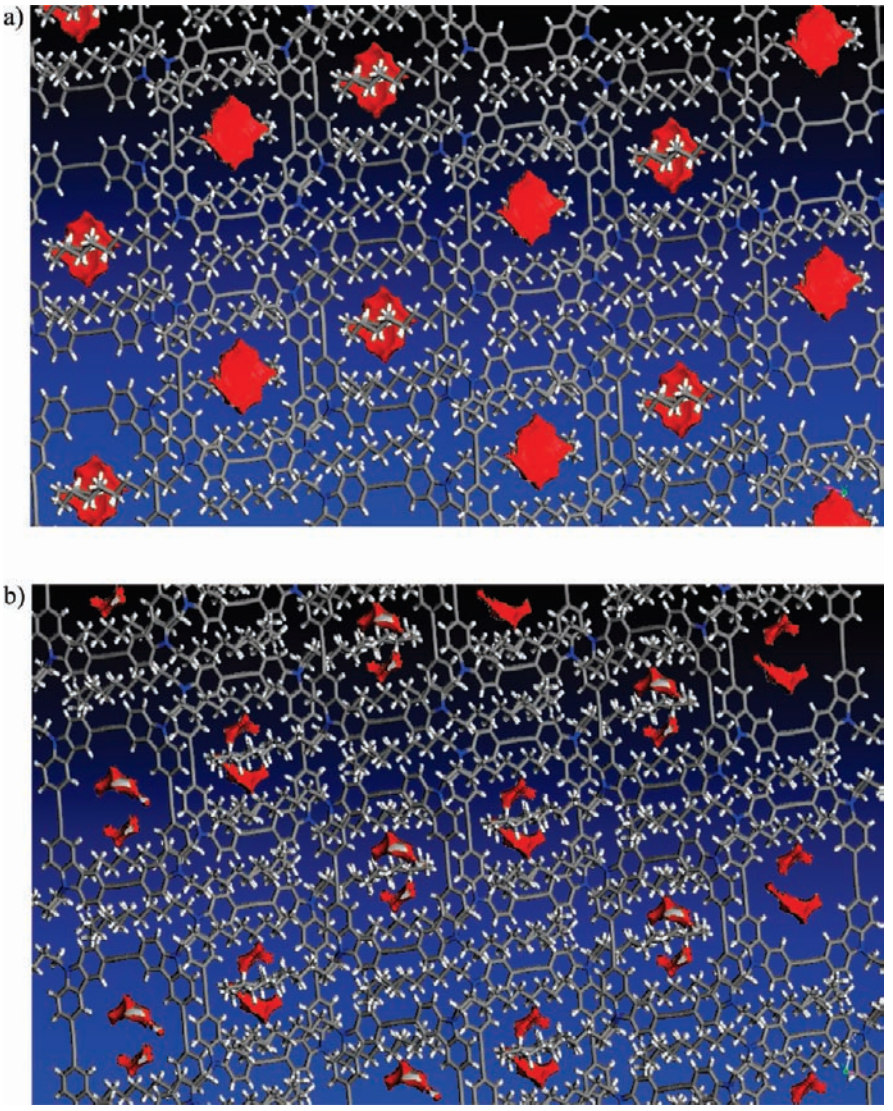

Figure 4. Visualization of the solvent volumes in (a) **2a**·DCM and (b) **2a**·MeOH. Solvent volumes are shown in red. The solvent void area in **2a**·MeOH is significantly smaller than that in **2a**·DCM as a result of the alkyl-chain disorder.

removed. Crystals of **2a**·MeOH crystallized in the space group $P2_1$, the same as in **2a**·DCM, with similar unit cell parameters; the unit cell volume of **2a**·MeOH ($V = 4094.8$ Å^3) is smaller than that of **2a**·DCM ($V = 4110.6$ Å^3) by only 15.8 Å^3.

Most notable in the structure of **2a**·MeOH is the extreme disorder of the alkyl chain C(67)−C(76), which is much more disordered than that in **2a**·**DCM** (see the Supporting Information). A model wherein the full alkyl chain is disordered about two positions with isotropic displacement restraints gave the best refinement. The disorder can be rationalized as follows. In the crystal, the disordered alkyl chains lie above and below the macrocycle cavity (Figure 3). The change in unit cell volume (15.8 Å^3) is less than the difference ΔV between the volume of two DCM molecules ($V_{DCM} = 76.8$ Å^3) and the volume of two MeOH molecules ($V_{MeOH} = 51.2$ Å^3):

$$\Delta V = 2(76.8\ \text{Å}^3 - 51.2\ \text{Å}^3) = 51.2\ \text{Å}^3$$

Thus, it is likely that the alkyl chains are disordered to account for the insufficient space-filling by MeOH. This may indicate that crystals of **2a** are indefinitely stable because alkyl-chain disorder prevents the destruction of the crystallinity. A visualization of the solvent volumes in **2a**·DCM and **2a**·MeOH (Figure 4) is illustrative: in **2a**·MeOH, the disordered alkyl chain appears to be responsible for the diminished void volume.

The morphology of **2b**, a polymorph of **2a**, is fascinating. The macrocycles in crystalline **2b** are arranged in the space group $C2/c$; half the macrocycle is related by inversion symmetry. As with **2a**, the macrocycle is mostly planar with a macrocycle plane deviation of 0.077 Å. The molecule as a whole again adopts a chairlike shape, and the overall packing motif is similar along the a and b axes. However, the packing along the c axis is not staggered as in **2a** but instead is aligned; this means that alkyl chains lie along the edges of the macrocycles rather than near the macrocycle cavities. This leads to contiguous solvent "channels" in the crystal, which propagate indefinitely along the b axis (Figure 5). The solvent channels are created by alternating rows of macrocycles and alkyl chains; there are significant interactions between the alkyl chains and macrocycles (~3.5 Å). The DCM solvent prevents the collapse of the alkyl chains into the cavities;

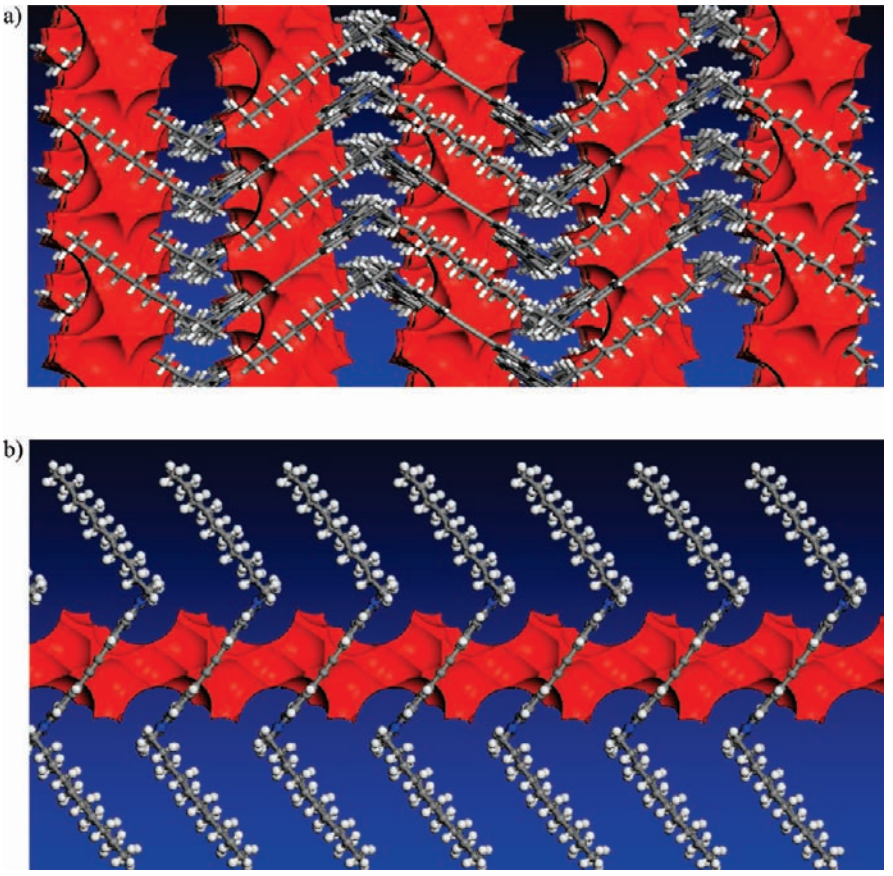

Figure 5. Visualization of the solvent channels in **2b**·DCM viewed down (a) the *a* axis and (b) the *c* axis. Solvent channels are shown in red.

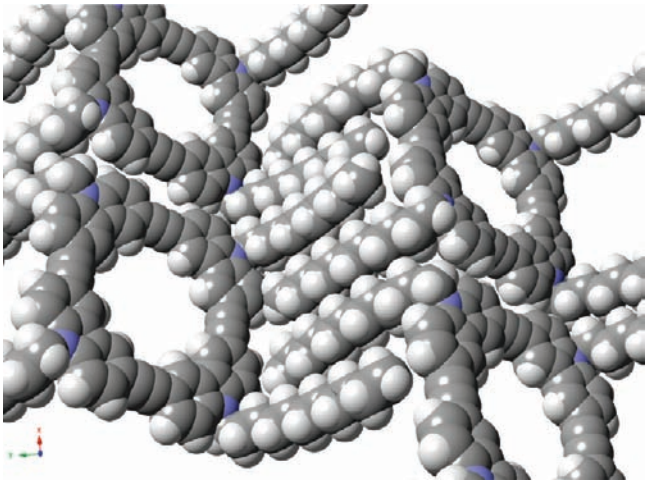

Figure 6. Space-filling representation of the banana-shaped distortion of the alkyl chains in **3**.

thus, when crystals of **2b** are removed from the solvent, the crystallinity is quickly lost. It is likely that collapse of **2b** leads to the packing motif seen in **2a**; however, we have not been able to verify that such a crystal-to-crystal transformation occurs.

It should be stressed that the crystals of **2a** and **2b** grew simultaneously under the same conditions. The remarkably large solvent channels present in **2b** are absent in **2a**; this should serve as a caveat that a single-crystal study may not tell the entire story of the solid-state chemistry of a novel material.[41]

Crystals of the C_{11}[4]cycle. In light of the fascinating morphologies we found above, it was of interest to see whether the packing arrangement of the C_{10}[4]cycle was unique to that particular alkyl-chain length. It should be noted that the length of an ordered C_{10} chain is approximately the same as the macrocycle's lateral N−N distance (11.435 and 12.298 Å, respectively). Large prisms of C_{11}[4]cycle **3** were grown following the general protocol. These plates crystallized in the monoclinic space group *Cc*. The packing morphology is very similar to that of **2a**, with a staggered arrangement along the *b* axis and A−B pleated sheets of macrocycles propagating along the *c* axis. This indicates that similar packing forces are in play for the C_{10} and C_{11} cases. However, unlike the case of **2a**, there is no solvent cavity present in **3** because of the longer alkyl chain. The ends of the alkyl chains are slightly distorted from the typical anti conformation, leading to a banana-shaped conformation (Figure 6). The slightly curved alkyl chains fill the macrocycle cavities, where in the case of **2a** and **2b** the cavities were filled with solvent. This further indicates that the staggered, pleated sheet arrangement is a favorable mode of packing for these macrocycles.

Crystals of the C_6[4]cycle. The effects of shorter alkyl chains on the solid-state packing were also investigated. The hexyl-substituted macrocycle **4** had the shortest alkyl chain that gave a macrocycle with any appreciable solubility. Slow diffusion of ether into a solution of **4** in DCM gave large prisms **4**·DCM. Crystals of **4**·DCM lost their crystallinity within hours of being removed from the solvent, indicative of a sensitive, solvated complex.

4·DCM crystallizes in the triclinic space group $P\bar{1}$. The macrocycles form ordered slip-stacks that run parallel to the axis

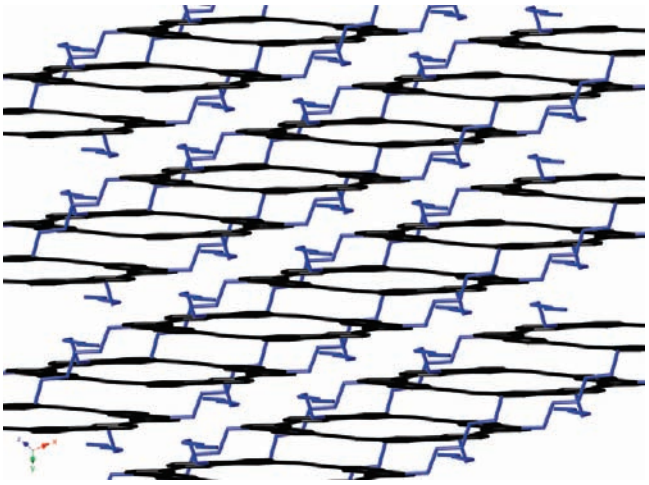

Figure 7. Packing of **4**·DCM viewed down [111]. H atoms and DCM molecules have been omitted for clarity.

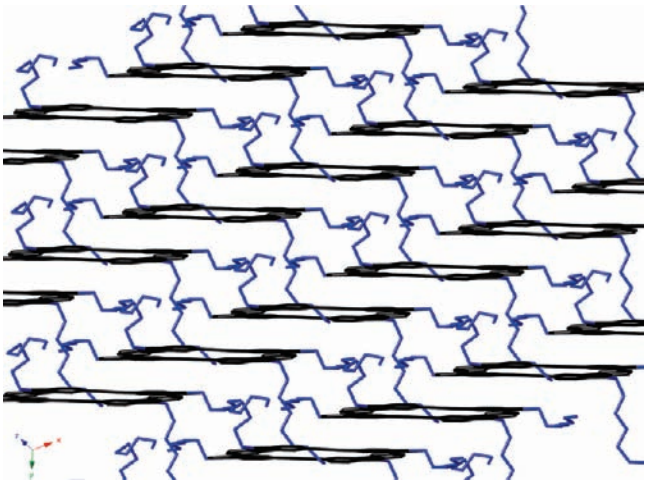

Figure 8. Packing of **5** viewed down [111]. H atoms have been omitted for clarity.

perpendicular to the [111] plane. In stark contrast to **2**, cofacial interactions between adjacent macrocycles dominate the packing motif, as indicated by the short distance between macrocycle planes (3.296 Å) (Figure 7). In contrast, the distance between two macrocycles in **2a** and **2b** is much longer (7.23 Å) as a result of the alternating alkyl chain/macrocycle packing. The presence of *ordered* DCM solvent in **4**·DCM is unique; as in the other crystals, DCM molecules were located within the cavities of the macrocycle. However, **4**·DCM was the only case in this study where positions for a guest solvent molecule could be acceptably refined. Hirschfeld surface analysis[42] indicated that close contacts from hydrogens in the DCM guest to the macrocycle host may be responsible for the ordered solvent.

Crystals of **4**·DCE were grown from diffusion of ether into a solution of **4** in 1,2-dichloroethane (DCE). The guest solvent was much more disordered in this case relative to **4**·DCM. Crystals of **4**·DCE are unique in that one of the carbazoles in the macrocycle is disordered away from the macrocycle plane. This causes the pendant alkyl chain to be disordered as well. This is likely an effect of the solvent molecule, as the disordered carbazole is adjacent to the solvent-containing cavity of another macrocycle and there appears to be close contact between that carbazole and DCE.

That cofacial aromatic−aromatic interactions become important as the alkyl-chain length decreases is a sensible explanation for the changes in crystal morphology in going from **2** and **3** to **4**. It is reasonable to assume that as these alkyl chains get shorter, aromatic interactions increasingly dominate the packing motif; upon complete removal of the alkyl chain, one may expect columnar architectures like those found in phenol-containing *m*-phenylene−ethynylene [6]cycles.[27] However, because of their low solubility, our attempts to prepare carbazole−ethynylene macrocycles with alkyl chains shorter than C_6 have to date been unsuccessful.

Crystals of the C_9[4]cycle. In an attempt to probe the "upper bound" between the intercalated packing in **2** and **3** and the cofacial arrangements seen in **4**, C_9[4]cycle **5** was prepared. In contrast to the examples shown above, crystallization of **5** was difficult; only very small plates of **5** were isolable. Macrocycle **5** crystallizes in the space group $P\bar{1}$; half the macrocycle is related by inversion symmetry. It contains an unusual disordering of two of the alkyl chains, resulting in two different orientations with 50% occupancy. While the macrocycle in the crystal is related by inversion symmetry, this alkyl chain is not; the alkyl chain and its inversion-related partner must have different orientations. Intercalation of one of the alkyl chains through the cavity of another macrocycle leads to the absence of guest solvent molecules in crystals of **5**.

The packing of **5** is similar to that of **4** (Figure 8), with aromatic cofacial interactions predominant. The packing of **5** indicates that there does appear to be an upper bound for the alkyl-chain length beyond which van der Waals interactions between alkyl chains and macrocycles dominate the packing motif.

DISCUSSION

Crystallographic investigations of SPMs are in high demand, not only because of the unique insights such investigations give but also because of the relative paucity of crystallographic data for such materials. Solid-state structure determination of SPMs are quite challenging for several reasons. Many systems do not crystallize at all; for example, attempts to grow single crystals of macrocycles containing **1** with pendant tetradecyl or $-CO_2C(CH_3)_2C_{11}H_{23}$ chains, both of which are of great interest because of their application as fluorescent sensors, have been unsuccessful. Crystalline SPMs having disordered alkyl chains often diffract poorly, leading to difficulties in their structure refinement. Furthermore, the shape persistence and large size of SPMs generally lead to the formation of cavities in which volatile, disordered solvent resides. Such "solvated" crystals, if not treated properly, may decompose in seconds upon removal from solution.[31]

The lamellar 2D aryl−alkyl arrangement seen in **2** and **3** is similar to a 2D motif that has been observed in scanning tunneling microscopy studies of square-shaped arylene−ethynylene macrocycles.[43] The relative order of the *n*-alkyl chains in these crystals is indicative of strong van der Waals interactions between alkyl groups in a sheet. In **2a**·DCM, for example, the distance between two parallel alkyl chains in one macrocycle is 12.5 Å, which is large enough to accommodate two more alkyl chains. These four alkyl chains are evenly spaced; the distance between hydrogens in adjacent alkyl chains is 2.6−2.9 Å. Clearly, the spacing of the alkyl chains as dictated by the size of the SPM

(12.2 Å to an edge) is optimal for this type of lamellar arrangement. The van der Waals interactions are maximized when the alkyl chains reach the approximate length of the macrocycle; the length of the C_{10} chain in **2a**·DCM is 12.2 Å, allowing for a regular arrangement.

In the course of the analysis of the above compounds, it became clear that the alkyl−aryl interactions present in crystals of **2** and **3** contribute significantly to the solid-state packing. Analysis of simulated powder diffraction data of the crystals indicated an unusual effect: the van der Waals interactions between the macrocycles and the alkyl chains present in **2** and **3** result in *d* spacings that closely resemble those for π stacking. The values of these *d* spacings deceptively appear to be associated with $\pi-\pi$ stacking, while in reality $\pi-\pi$ stacking does not exist in these solids!

The simulated powder diffraction data for the crystals illustrate this phenomenon. In all cases, the Miller plane that corresponds to the *d* spacing of ∼3.5 Å is an intense reflection in the powder data. However, in the case of the staggered alkyl−aryl motif present in **2** and **3**, there *also* exists a reflection at double this *d* spacing that corresponds to the actual *d* spacing between aromatic macrocycles [except in **2b**, where the (*h*/2, *k*/2, *l*/2) peak is systematically absent]. In the cases where aromatic π stacking is present, the (*h*/2, *k*/2, *l*/2) reflection does not exist. Thus, the presence of a reflection at 2*d* in the powder diffraction data is indicative of staggered layers, that is, layers consisting of alkyl chains followed by layers consisting of aromatic rings (however, as indicated by the systematic absences seen in **2b**, the reverse is *not* true). We were able to confirm this experimentally with powder diffraction data for crystalline **3** (see the Supporting Information). Crystals of macrocycle **3** are easily grown in large quantities and are sufficiently stable that they could be ground for the powder diffraction experiment. Using the single-crystal data for **3**, we were able to index the reflections in the powder diffraction data for **3**. We found that the reflection at *d* = 3.62 Å corresponds to the Miller plane parallel to alternating layers of macrocycles and alkyl chains. As expected, there was also a peak at 2*d* = 7.24 Å corresponding to the distance between layers of macrocycles. Therefore, powder diffraction data can be used to determine the presence of staggered versus cofacial packing motifs in cases where single crystals cannot be grown.

The C_{14}[4] cycle **6** was prepared previously by us; however, as stated above, we were unable to grow crystals suitable for single-crystal analysis. Nonetheless, polycrystalline **6** was readily obtained by growth from slow diffusion of ethyl acetate into a DCM solution, and the resulting powder was analyzed by X-ray diffraction (see the Supporting Information). The presence of a staggered packing arrangement was apparent from the powder diffraction data, according to the observations above. An intense peak at *d* = 3.62 Å was present, as well as a peak at 2*d* = 7.24 Å; thus, we predict a staggered alkyl/aromatic packing arrangement in the case of polycrystalline **6**.

CONCLUSION

An extensive crystallographic analysis of macrocycles **1** with varying alkyl-chain lengths has been carried out. The alternating alkyl/aryl packing motif seen in crystals of **2** and **3** is unique and appears to be the result of maximization of the van der Waals interactions between the alkyl chains and aromatic parts of the macrocycles. The packing of systems with less than C_{10} side chains is dominated by aromatic−aromatic interactions. As evidenced by **2a** and **2b**, polymorphism of large aromatic systems may belie the full story of the solid-state chemistry of a novel material. Additionally, correlating the powder and single-crystal X-ray diffraction data for **6** has enabled us to suggest that its solid-state structure is similar to that of **2** and **3.** Additional crystallographic studies on various arylene−ethynylene macrocycles should give a more complete picture of the nature of these interesting materials and shed light on their functional properties.

ASSOCIATED CONTENT

Supporting Information. Synthetic procedures and characterization for all compounds, crystallographic data for **2**−**5** (CIF), and powder diffraction data for **3** and **6**. This material is available free of charge via the Internet at http://pubs.acs.org.

AUTHOR INFORMATION

Corresponding Author
jsmoore@illinois.edu

Present Addresses
[†]ETH-Zürich, Hönggerberg, CH-8093 Zürich, Switzerland.

ACKNOWLEDGMENT

This work was supported by the National Science Foundation (CHE-1010680). The Materials Chemistry Laboratory at the University of Illinois was supported in part by Grants NSF CHE 95-03145 and NSF CHE 03-43032 from the National Science Foundation. The authors thank Dr. Danielle Gray (Materials Chemistry Laboratory, University of Illinois) and Charlotte Stern and Dr. Amy Sarjeant (Northwestern University) for helpful discussions and assistance with single-crystal and powder X-ray diffraction experiments.

REFERENCES

(1) Loser, S.; Bruns, C. J.; Miyauchi, H.; Ortiz, R. P.; Faccetti, A.; Stupp, S. I.; Marks, T. J. *J. Am. Chem. Soc.* **2011**, *133*, 8142.
(2) Walker, B.; Kim, C.; Nguyen, T.-Q. *Chem. Mater.* **2011**, *23*, 470.
(3) Anthony, J. E. *Chem. Mater.* **2011**, *23*, 583.
(4) Roncali, J. *Acc. Chem. Res.* **2009**, *42*, 1719.
(5) Kivala, M.; Diederich, F. *Acc. Chem. Res.* **2009**, *42*, 235.
(6) Nakanashi, W.; Yoshioka, T.; Taka, H.; Xue, J. Y.; Kita, H.; Isobe, H. *Angew. Chem., Int. Ed.* **2011**, *50*, 5323.
(7) Moore, J. S. *Acc. Chem. Res.* **1997**, *30*, 402.
(8) Watson, M. D.; Fechtenkötter, A.; Müllen, K. *Chem. Rev.* **2001**, *101*, 1267.
(9) Pasini, D.; Ricci, M. *Curr. Org. Synth.* **2007**, *4*, 59.
(10) Grave, C.; Schlüter, A. D. *Eur. J. Org. Chem.* **2002**, 3075.
(11) Tahara, K.; Tobe, Y. *Chem. Rev.* **2006**, *106*, 5274.
(12) Zhang, W.; Moore, J. S. *Angew. Chem., Int. Ed.* **2006**, *45*, 4416.
(13) Feng, W.; Yamato, K.; Yang, L.; Ferguson, J. S.; Zhong, L.; Zou, S.; Yuan, L.; Zeng, X. C.; Gong, B. *J. Am. Chem. Soc.* **2009**, *131*, 2629.
(14) MacLachlan, M. J. *Pure Appl. Chem.* **2006**, *78*, 873.
(15) Gross, D. E.; Moore, J. S. *Macromolecules* **2011**, *44*, 3685.
(16) Rowan, S. J.; Cantrill, S. J.; Cousins, G. R. L.; Sanders, J. K. M.; Stoddart, J. F. *Angew. Chem., Int. Ed.* **2002**, *41*, 898.
(17) Mastalerz, M. *Angew. Chem., Int. Ed.* **2010**, *49*, 5042.
(18) Ge, P.-H.; Fu, W.; Herrmann, W. A.; Herdtweck, E.; Campana, C.; Adams, R. D.; Bunz, U. H. F. *Angew. Chem., Int. Ed.* **2000**, *39*, 3607.

(19) Pschirer, N. G.; Fu, W.; Adams, R. D.; Bunz, U. H. F. *Chem. Commun.* **2000**, 87.
(20) Zhang, W.; Brombosz, S. M.; Mendoza, J. L.; Moore, J. S. *J. Org. Chem.* **2005**, *70*, 10198.
(21) Zhang, W.; Moore, J. S. *J. Am. Chem. Soc.* **2004**, *126*, 12796.
(22) Zhang, W.; Moore, J. S. *J. Am. Chem. Soc.* **2005**, *127*, 11863.
(23) Hoeben, F. J. M.; Jonkheijm, P.; Meijer, E. W.; Schenning, A. P. H. J. *Chem. Rev.* **2005**, *105*, 1491.
(24) Moulton, B.; Zaworotko, M. J. *Chem. Rev.* **2001**, *101*, 1629.
(25) Anthony, J. E.; Brooks, J. S.; Eaton, D. L.; Parkin, S. R. *J. Am. Chem. Soc.* **2001**, *123*, 9482.
(26) Anthony, J. E.; Eaton, D. L.; Parkin, S. R. *Org. Lett.* **2002**, *4*, 15.
(27) Venkataraman, D.; Lee, S.; Zhang, J.; Moore, J. S. *Nature* **1994**, *371*, 591.
(28) Kawase, T.; Ueda, N.; Darabi, H. R.; Oda, M. *Angew. Chem., Int. Ed. Engl.* **1996**, *35*, 1556.
(29) Höger, S.; Enkelmann, V.; Bonrad, K.; Tschierske, C. *Angew. Chem., Int. Ed.* **2000**, *39*, 2267.
(30) Hosokawa, Y.; Kawase, T.; Oda, M. *Chem. Commun.* **2001**, 1948.
(31) Müller, P.; Uson, I.; Hensel, V.; Schlüter, A.-D.; Sheldrick, G. M. *Helv. Chim. Acta* **2001**, *84*, 778.
(32) Höger, S.; Morrison, D. L.; Enkelmann, V. *J. Am. Chem. Soc.* **2002**, *124*, 6734.
(33) Grave, C.; Lentz, D.; Schäfer, A.; Samori, P.; Rabe, J. P.; Franke, P.; Schlüter, A.-D. *J. Am. Chem. Soc.* **2003**, *125*, 6907.
(34) Traber, B.; Oeser, T.; Gleiter, R. *Eur. J. Org. Chem.* **2005**, 1283.
(35) Naddo, T.; Che, Y.; Zhang, W.; Balakrishnan, K.; Yang, X.; Yen, M.; Zhao, J.; Moore, J. S.; Zang, L. *J. Am. Chem. Soc.* **2007**, *129*, 6978.
(36) Bindl, M.; Stade, R.; Heilmann, E. K.; Picot, A.; Goddard, R.; Fürstner, A. *J. Am. Chem. Soc.* **2009**, *131*, 9468.
(37) Heppekausen, J.; Stade, R.; Goddard, R.; Fürstner, A. *J. Am. Chem. Soc.* **2010**, *132*, 11045.
(38) It should be noted that the solvent was quite ordered in **3**, as reflected by the quality of the data collected using Mo radiation.
(39) The macrocycle plane is defined as the least-squares plane of the non-hydrogen atoms of the macrocycle, not including the pendant alkyl chains; the macrocycle plane deviation is the standard deviation for all of the atoms that define this plane.
(40) Spek, A. L. *J. Appl. Crystallogr.* **2003**, *36*, 7.
(41) Dunitz, J. D.; Bernstein, J. *Acc. Chem. Res.* **1995**, *28*, 193.
(42) Spackman, M. A.; Jayatilaka, D. *CrystEngComm* **2009**, *11*, 19.
(43) Tahara, K.; Lei, S.; Mamdouh, W.; Yamaguchi, Y.; Ichikawa, T.; Uji-i, H.; Sonoda, M.; Hirose, K.; De Schryver, F. C.; De Feyter, S.; Tobe, Y. *J. Am. Chem. Soc.* **2008**, *130*, 6666.